

Effect of construction sequence on three-arch tunnel behavior-Numerical investigation

C. Yoo* and J. Choi^a

School of Civil and Architectural Engineering, Sungkyunkwan University, Suwon, Korea

(Received May 14, 2017, Revised February 13, 2018, Accepted March 23, 2018)

Abstract. This paper concerns a numerical investigation on the effect of construction sequence on three-arch (3-Arch) tunnel behavior. A three-arch tunnel section adopted in a railway tunnel construction site was considered in this study. A calibrated 3D finite element model was used to conduct a parametric study on a variety of construction scenarios. The results of analyses were examined in terms of tunnel and ground surface settlements, shotcrete lining stresses, loads and stresses developed in center column in relation to the tunnel construction sequence. In particular, the effect of the side tunnel construction sequence on the structural performance of the center structure was fully examined. The results indicated that the load, thus stress, in the center structure can be smaller when excavating two side tunnels from opposite direction than excavating in the same direction. Also revealed was that no face lagging distance between the two side tunnels impose less ground load to the center structure. Fundamental governing mechanism of three-arch tunnel behavior is also discussed based on the results.

Keywords: 3-arch tunnel; 3D finite element analysis; construction sequence; face lagging distance; center column load

1. Introduction

Two-arch or three-arch tunnels are typically adopted when a large cross section is required, e.g., underground railway station. Due to rather complex sequential construction procedures, the behavior of these tunnels is somewhat different from that of a single tube tunnel. A number of structural problems in two or three arch tunnels such as crack development in the center column have been reported (Kim *et al.* 2016). For safe execution of a three-arch tunnel construction, it is essential to fully understand the behavior of 3-Arch tunnel in relation to construction sequence.

Surprisingly, relevant studies on this subject are scarce. Masaki *et al.* (2007) conducted a study on large double adjoined binocular tunnels at densely residential area and reported fundamental mechanism on the behavior of large section adjoined tunnels. Oh (2007) investigated the fundamental mechanism of center column load development during the 2-Arch tunnel excavation and proposed a method for predicting the column load. A good comparison between the proposed method and those from the empirical formula suggested by Matsuda (1997) was reported.

Later, Keisuke *et al.* (2008) investigated a three-arch tunnel behavior constructed in heavily populated area using the measured data. In this study, the excavation method and center column load were thoroughly analyzed in order to ensure the stability of large cross section tunnels. Myoung

(2008) performed a 2D finite element study on a number of construction scenarios of two-arch tunnel and the results were compared to identify the effect of construction sequence on the tunnel behavior. More recently, Yoo *et al.* (2009) investigated the three-dimensional behavior of two-arch tunnels using a calibrated 3D finite element model. Based on the results, the deformation behavior as well as the center column load were fully investigated. Although the aforementioned studies have provided insights into the behavior of multi-arch tunnel behavior, much still needs to be investigated in order to fully understand the fundamental governing mechanism in terms of the effect of construction sequence on the three-arch tunnel behavior.

In this paper, the behavior of three-arch tunnels constructed in difficult ground conditions is investigated. A three-arch tunnel section adopted in a railway tunnel construction site was considered in this study. A calibrated 3D finite element model was used to conduct a parametric study on a variety of construction scenarios. The 3D finite element numerical modeling approach was adopted as a tool in carrying out this investigation as it has been successfully used in previous studies on tunneling (Lee *et al.* 2016, Yoo 2016, Zidan and Ramadan 2018).

The results of analyses were examined in terms of the tunnel deformation, shotcrete lining stresses, and loads on the center column in relation to the side tunnel construction sequence. This paper describes the tunneling condition, the 3D finite element model, and the results of the parametric study.

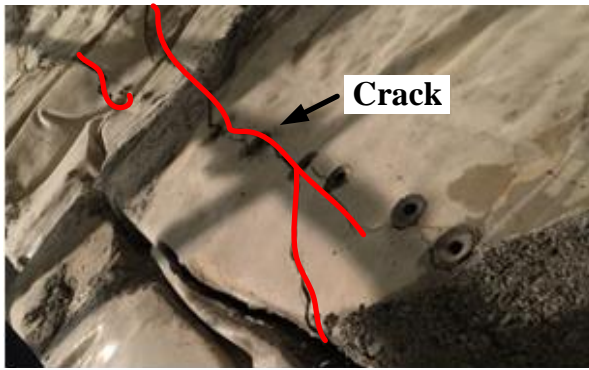
2. Typical three-arch tunnel damage

2.1 Crack development in center structure

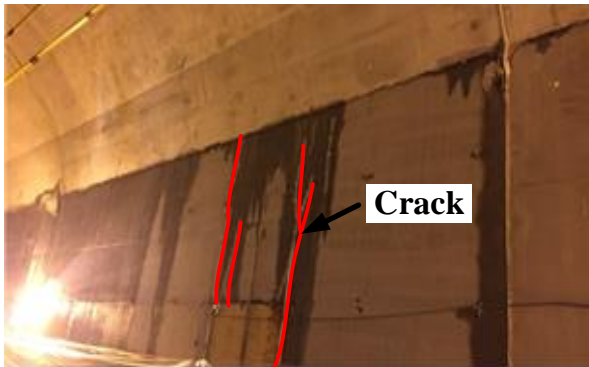
*Corresponding author, Professor

E-mail: csyoo@skku.edu

^aFormer Ph.D. Student



(a) Cracks on concrete lining



(b) Cracks on center column

Fig. 1 Structural damage in a three-arch tunnel structure

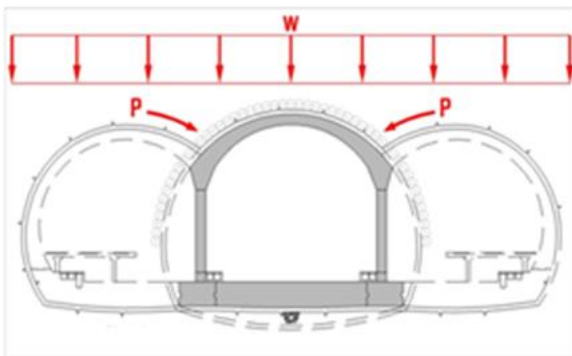


Fig. 2 Load transfer mechanism on center column of three-arch tunnel

Structural tunnel damages in concrete lining have been reported in recently constructed three-arch tunnels of Sooseo-Pyungtaek high speed railway line. The structural damages include cracks in concrete lining and center column. Fig. 1 show photos of typical crack development in the central structure after the placement of concrete lining. Execution of remedial work and associated construction delay resulted in significant economic loss. In order to prevent such problems from happening, thorough understanding of the load transfer mechanism during the three-arch tunnel construction is essential.

Fig. 2 shows a conceptual load transfer mechanism on the center structure during a three-arch tunnel excavation. As shown, a structural arch with center column is first constructed immediately after the center tunnel excavation. For a given ground condition, the load on the center

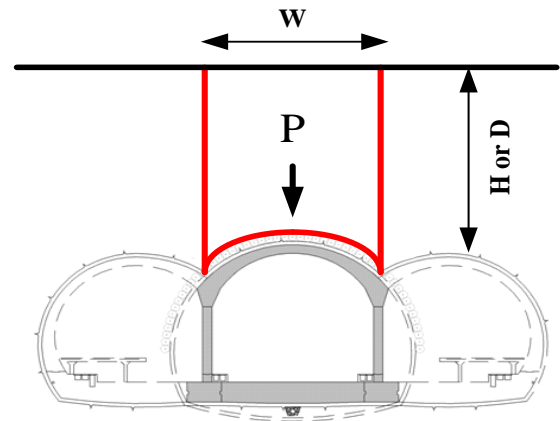


Fig. 3 Conceptual diagram of Mastuda (1997) approach

structure is thus strongly influenced by the ground load transfer during excavation from the two side tunnels. As the center structure is constructed immediately after the center tunnel excavation, the center structure needs to be designed so as to support the ground load resulting from the two side tunnel excavation.

In view of the center structure design, it is of utter most importance to accurately estimate the exerting load on the center structure. Inappropriate estimation of the center structure load may lead to cracks in combination of other construction related load such as blasting load in cases of rock tunnels.

2.2 Center column load calculation method

As mentioned in the previous section, it is important to correctly consider the load acting on the center structure in order to ensure the overall tunnel stability for a design perspective. Generally, for design of two- or three-arch tunnels, the load acting on the center structure P with reference to Fig. 3 is computed either by empirical approaches or numerical approach.

The simplified method suggested by Matsuda (1997) of the traditional arching theory based loosened load concept is used for soft ground and rock, respectively. In case of the simplified method by Matsuda (1997), the load acting on the center structure P is computed as $P = \gamma \times D \times W$ when the cover depth (H) is larger than the tunnel diameter (D) or $P = \gamma \times H \times W$ otherwise. In this approach, the input parameters are rather simple, such as topography, unit weight and tunnel width. This approach is known to be somewhat conservative. The conservativeness of this approach can be eliminated by adopting a reduction factor proposed by Oh (2007).

The numerical approach is a bit more rigorous method which requires to estimate displacements of the center structure using a continuum analysis. The calculated displacements in each construction step are then used as boundary loads in a ring-beam structural model. In this way, it is possible to compute the section forces at a corresponding step. Details of the numerical approach is beyond the scope of this paper and therefore will not be discussed further.

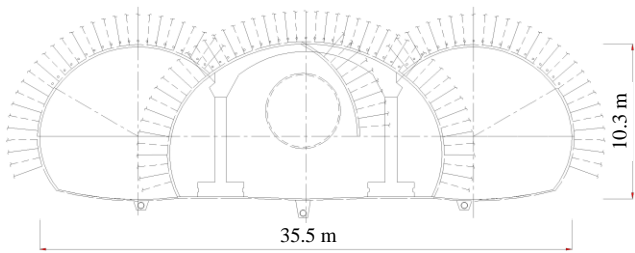


Fig. 4 Cross section of three-arch tunnel considered

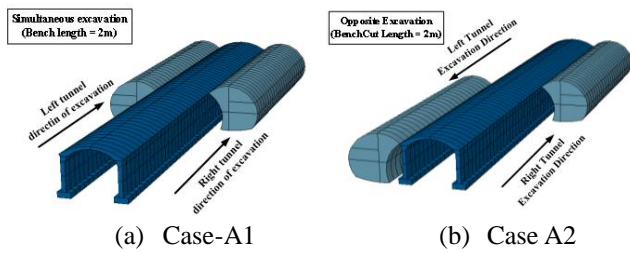


Fig. 5 Schematic representation of Series A

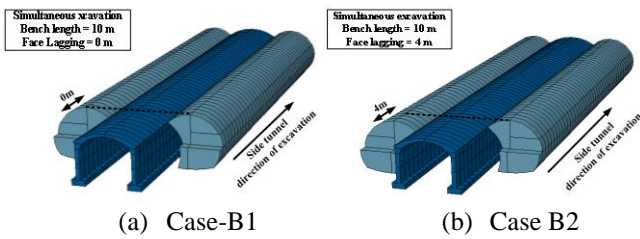


Fig. 6 Schematic representation of Series B

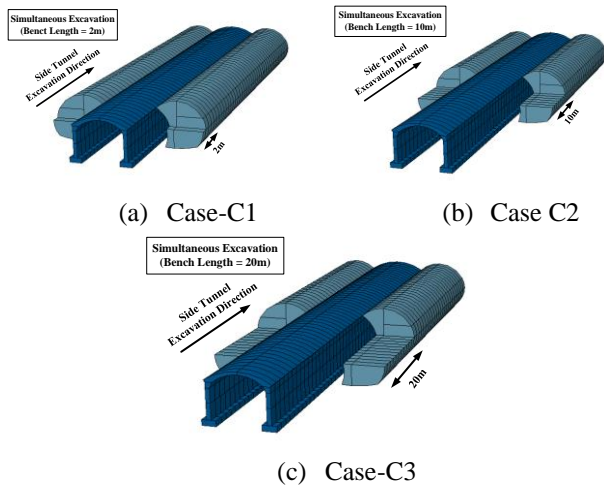


Fig. 7 Schematic representation of Series C

Table 1 Summary of Series considered

Series	Excavation direction	Bench length (m)	Face lagging (m)
A	A1	same	2
	A2	opposite	2
B	B1	same	0
	B2	same	4
C	C1	2	0
C	C2	10	0
C	C3	20	0

3. Tunneling cases considered

3.1 Tunnel geometry

In this study, a three-arch tunnel having a cover depth of 30 m was considered, the schematic diagram of which is shown in Fig. 4. Note that the tunnel section considered is the one adopted in Lot 000 for Sooseo-Pyungtaek high speed railway line (named SRT Line hereunder) construction site.

The tunnel was assumed to be constructed in a uniform ground of rock class V as per RMR classification, which can be considered unfavorable ground condition when considering the large tunnel section. With reference to Fig. 4, the three-arch tunnel section has a total excavation width (D_t) and height (H) of approximately 35.5 and 10.3 m, respectively, with a center tunnel having a diameter (D) of 10 m.

The primary support of the tunnel consists of 5 m long rock bolts, installed at 5 m center-to-center spacing, together with 160 mm thick shotcrete. The center structure, which is constructed immediately after the center tunnel excavation, consists of 300 mm thick concrete arch and 800 mm thick two longitudinally continuous columns. Although auxiliary methods such as fore poling and pipe umbrella techniques are implemented in this type of tunneling condition, they are not considered for the sake of simplicity.

In terms of the construction sequence, the center tunnel excavation proceeds first, followed by the construction of the center structure. The left and right-side tunnels are then excavated with the bench cut method.

3.2 Construction sequences considered

Three series of construction scenarios were developed to investigate the effect of excavation sequence of side tunnels on the tunnel/ground deformation and structural performance of the center structure. *Series A* considers the effect of excavation direction of two side tunnels. In *Series B*, the effect of face lagging distance between the two side tunnels was the main focus. Finally, *Series C* concerns the effect of bench length. It should be noted that *Series A* and *B* the bench length was kept constant at 2 m while no face lagging between the right and left side tunnels was considered in *Series C*. Figs. 5-7 show schematic representation of the series analyzed. Details of each series are summarized in Table 1.

4. Three-dimensional finite element analysis

4.1 3D finite element model

In this study, a commercial finite element (FE) program Abaqus 6.16 (Abaqus 2016) was used, which is a multi-purpose FE package that can be applied to various engineering fields, such as civil and mechanical engineering. Abaqus provides a variety of soil constitutive models and is known to be effective in simulating tunneling problems which involve stepwise construction process.

Fig. 8 shows a typical finite element model, with relevant dimensions, adopted in the analysis. In terms of the displacement boundary condition, roller boundaries are

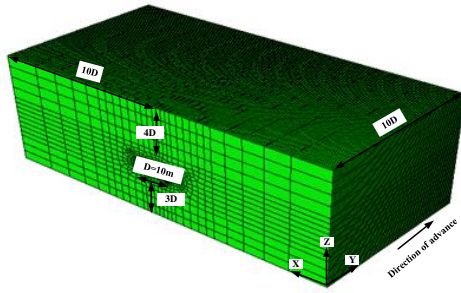


Fig. 8 Finite element model

Table 2 Material properties adopted in analysis

Parameters	γ (kN/m ³)	c (kPa)	ϕ/ψ (deg)	E (MPa)	ν
Ground	23	100	35/10	5000	0.3
Shotcrete	25	-	-	10000	0.2
Rock bolt	78.5	-	-	210000	0.2

* γ = unit weight; c = cohesion; ϕ = internal friction angle; ψ = dilation angle; E =Young's modulus; ν = Poisson's ratio

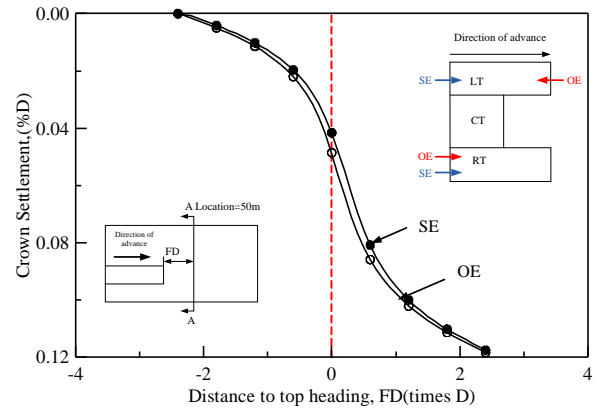
placed on the vertical faces of the mesh, i.e., $U_x = 0$ or $U_y = 0$, while fixed boundary condition, i.e., $U_x = U_y = U_z = 0$ is applied at the bottom. As shown, the left and right boundaries are located at about 10D ($D = 10\text{m}$) from the center of the tunnel and the lower boundary is located at about 3D below the tunnel invert.

4.2 Discretization and constitutive modeling

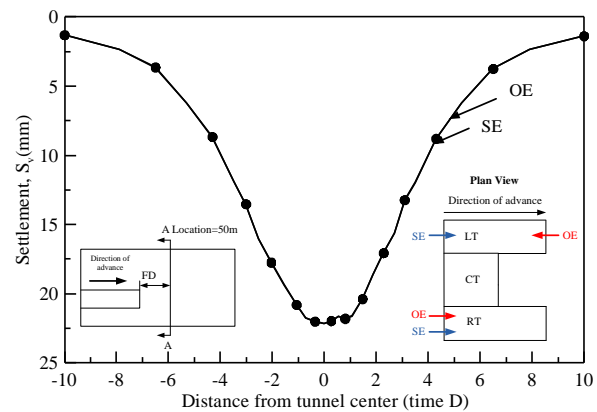
Eight-node brick element with reduced integration (C3D4R) was used to discretize the ground while truss element (T3D2) and four-node shell element (S4R) element were used for rock bolts and shotcrete lining, respectively. With regard to the constitutive modeling, the ground was assumed to be an elasto-plastic material conforming to the Mohr-Coulomb failure criterion together with the non-associated flow rule proposed by Davis (1968), while the shotcrete lining and rock bolt were assumed to behave in a linear elastic manner. The time dependency of the strength and stiffness of the shotcrete lining after installation was not modeled in the analysis, but rather an average value of Young's modulus of 10 GPa, representing green and hard shotcrete conditions reported in literature (Queiroz *et al.* 2006), was employed. Table 2 summarizes the mechanical properties of the materials used in the analyses. Note that these values were taken from a design document (Korea Rail Network Authority 2012).

The construction sequence described in Figs. 5-7 for each case was closely followed in the finite element modeling. It should however be noted that although the center tunnel excavation adopts the center diaphragm excavation method in the actual tunneling sequence, the center diaphragm wall was not explicitly modeled for the sake of modeling simplicity.

The above 3D numerical modeling strategy adopted in this paper has been validated by Yoo (2009) although limited. Details of the validation can be found in Yoo (2009)



(a) Center tunnel crown settlement



(b) Transverse surface settlement

Fig. 9 Variation of center tunnel deformation and transverse surface settlement for Series A

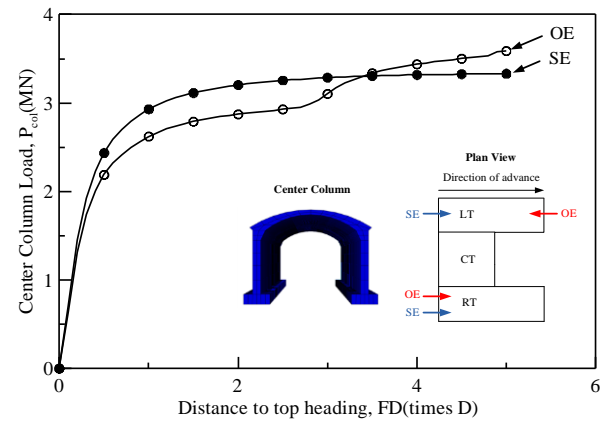


Fig. 10 Variation of progressive development of center column load for Series A

5. Results and discussion

In this section, the results such as tunnel deformation, surface settlement, and column load (stress) are related to the excavation sequence. For example, the progressive development of these results is given in relation to the location of the top heading of side tunnel normalized by the center tunnel diameter as FD . In addition, the center column load was obtained by multiplying the vertical stress in the column by the appropriate cross-sectional area. The center column load is in fact the load that needs to be

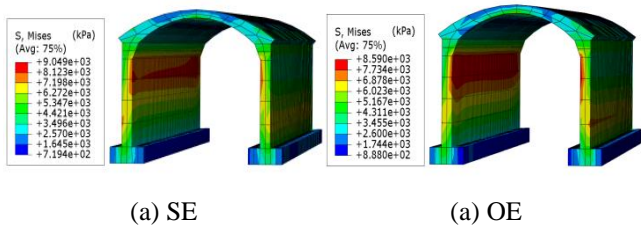


Fig. 11 von Mises stresses in center column for Series A

supported by the center structure constructed immediately after the center tunnel.

5.1 Effect of side tunnel excavation direction

The effect of side tunnel excavation sequence, i.e., simultaneous versus opposite direction excavation, on the tunneling performance are examined with emphasis on the tunnel deformation and the structural performance of the center structure using Series A analysis. In Series A, the top and lower bench length was fixed at 2 m.

Fig. 9 shows the time history plot of crown settlement of the center structure caused by the side tunnel excavation and the transverse settlement trough at the ground surface due to the center as well as the side tunnel excavation. As shown in Fig. 9(a) the crown settlement history plot does not seem to greatly change with the side tunnel excavation direction showing almost identical settlement history plots. The transverse surface settlement plots in Fig. 9(b) also show identical troughs confirming that the side tunnel excavation direction during the three-arch tunnel construction has negligible effect on the tunneling performance.

Fig. 10 shows the effect of side tunnel excavation direction on the progressive development of the vertical load in the center column. As shown, the column load sharply increases as the side tunnel excavation commences after which it converges to approximately 2.3-3.2 MN, depending on the excavation direction, i.e., same (SE) or opposite (OE) direction. It is worth noting that a sudden increase in the column load occurs when crossing the top headings of the both excavations for opposite excavation (OE), leading to a larger column load than the same excavation direction case. In terms of the magnitude, the final column load seems to be 10% larger in the same direction excavation (SE) than the opposite direction excavation (OE). Although further studies are required to arrive at a general conclusion, these results suggest that it is advantageous to excavate the side tunnels in opposite direction in view of the load on the center structure. Fig. 11 compares contour plots of von Mises stress in the center column upon completion of side tunnel excavation for the two excavation direction cases of side tunnels, i.e., OE and SE. The opposite direction excavation tends to yield a wider stress concentrated zone in the shoulder area, although the stress level is a bit smaller, supporting the results in Fig. 11.

It can therefore be concluded that to execute the side tunnel excavation in the same direction would be more beneficial in view of the structural load (or stress) developed in the center column.

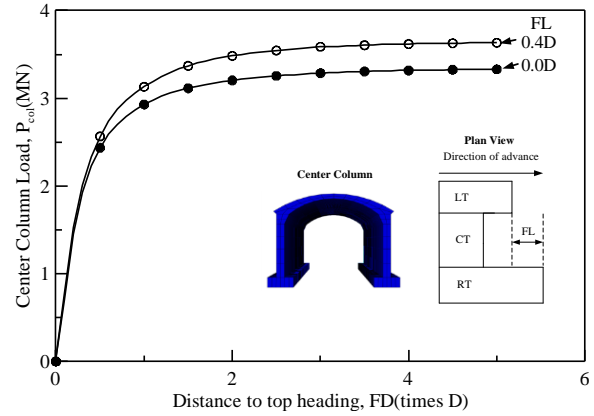


Fig. 12 Variation of progressive development of center column load for Series B

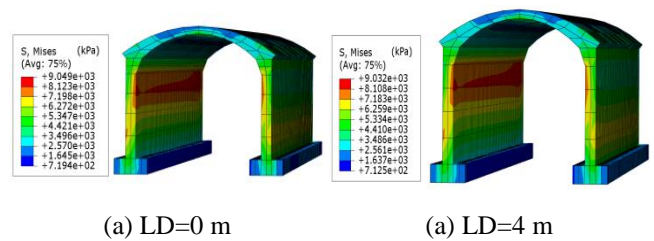
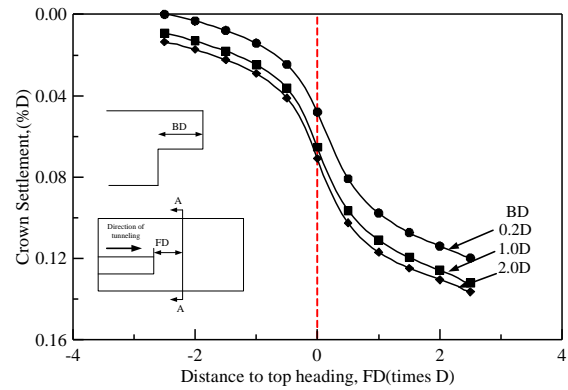
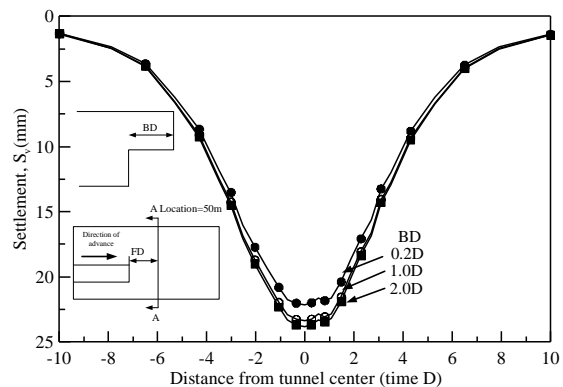


Fig. 13 von Mises stresses in center column for Series B



(a) Center tunnel crown settlement



(b) Transverse surface settlement

Fig. 14 Variation of center tunnel deformation and transverse surface settlement for Series C

5.2 Effect of face lagging distance of side tunnels

Based on the results from Series B, the effect of face

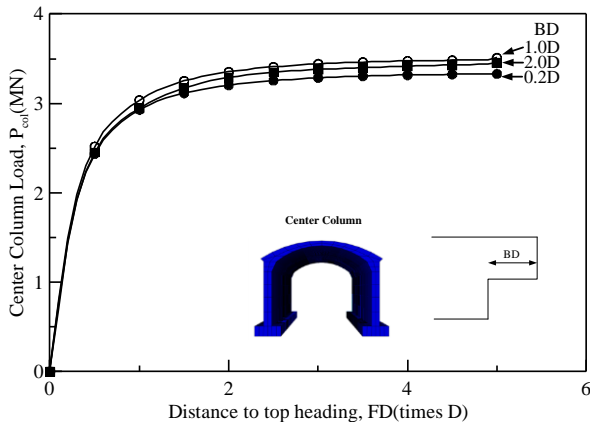


Fig. 15 Variation of progressive development of center column load for Series C

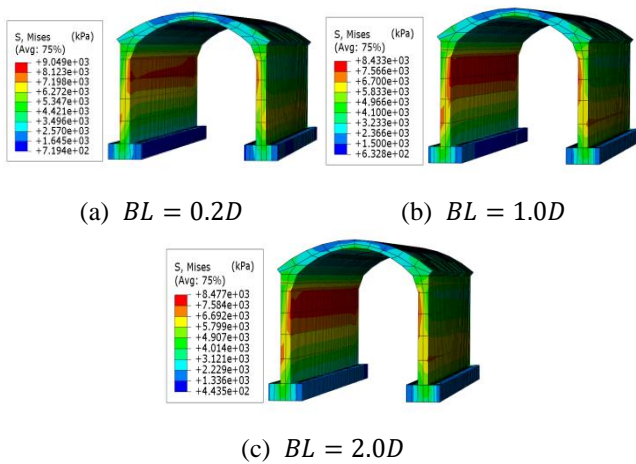


Fig. 16 von Mises stresses in center column for Series C

lagging distance of side tunnels is examined. It is intuitively expected that the longer the face lagging distance, the less is the impact of side tunnel excavation on the center structure. The results are shown in Figs. 12 and 13. The tunnel deformation as well as transverse surface settlements are basically not influenced by the face lagging distance and therefore not shown here.

Shown in Fig. 12 is the progressive development of center column load for two face lagging distances, i.e., $FL = 0\text{ m}$ (no face lagging) and $FL = 4\text{ m}$. Surprisingly, the greater the face lagging case, the larger is the column load. Although not clearly seen, such a trend is also reflected in the contour plots of von Mises stresses presented in Fig. 13. The reason for such a trend may be attributed to the load sharing mechanism between the ground and the center structure during side tunnel excavation. Further study is required to confirm the finding.

5.3 Effect of bench length of side tunnel excavation

The effect of bench length of side tunnel excavation is shown in Figs. 13-16. Note here that the two side tunnels have the same face advancing direction. As can be observed, Fig. 13 shows that the center tunnel crown

settlement as well as surface settlement tend to increase as the bench length (BL) increases, although the differences are not significant. This suggests that early ringing closure results in smaller tunnel deformation as in single tunnel excavation.

The variation of the center column load with the bench length of side tunnel excavation is shown in Fig. 14. Similar to the trend observed in the tunnel and ground deformation, an increase in the bench length seems to increase the center column load as well, although minimal. The contour plots of von Mises stresses shown in Fig. 15 also confirm the observation. Such a trend implies that the ground load transfer to the center column during the side tunnel excavation can be reduced by keeping the bench length to a minimum.

6. Conclusions

In this paper, the results of a numerical investigation on the effect of three-arch tunnel construction sequence on the tunnel and ground deformations and the structural performance of center structure are presented. A three-arch tunnel section adopted in a railway tunnel construction site was considered in this study. A calibrated 3D finite element model was used to conduct a parametric study on a variety of construction scenarios. The results of analyses were examined in terms of tunnel and ground deformation as well as the center column load in relation to the side tunnel construction sequence. Based on the findings the following conclusions can be drawn, although limited to the cases considered in this study.

- 1) Excavation direction of each side tunnel has essentially no influence on the tunnel deformation as well as the surface settlement while the center column load is smaller when two side tunnels are excavated in opposite direction
- 2) Face lagging distance between two side tunnels also does not have appreciable effect on the tunnel deformation as well as the surface ground settlement. However, the face lagging distance affects the column load such that the greater the face lagging, the larger is the column load, suggesting that keeping the face lagging distance to minimum may be more beneficial in view of the center tunnel performance.
- 3) The center tunnel crown settlement as well as surface settlement tend to increase as the bench length increases. Similarly, an increase in the bench length increases the center column load.

In short, the results of the numerical investigation suggest that the excavation sequence of side tunnels during three arch tunnel construction influences more on the load developed in the center structure than on the tunnel as well as ground deformation. It is shown that some economic benefit in terms of the center column section can be achieved by selecting appropriate side tunnel excavation sequence so as to minimize the center column load,

Acknowledgements

This research is supported by the Korea Agency for

Infrastructure Technology Advancement under the Ministry of Land, Infrastructure and Transport of the Korean government (Project Number: 16SCIP-B108153-02). The financial support is gratefully acknowledged.

References

- Abaqus. (2016), *User's Manual Version 6.16*, Hibbitt, Karlsson, and Sorensen, Inc., Pawtucket, Rhode Island, U.S.A.
- Davis, E.H. (1968), *Theories of Plasticity and the Failure of Soil Masses*, in *Soil Mechanics: Selected Topics*, Butterworth, London, U.K., 341-380.
- Keisuke, T., Maresuke, M., Yasuki, A., Motoyoshi O. and Masashi, K. (2008), "Measurement in large double adjoined binocular tunnels at densely residential area", *Jap. Civ. Eng. Soc. Tunn. Eng. Committee*, **18**, 63-70.
- Korea Rail Network Authority. (2012), *Gyeongbu High Speed Railway Lot No. 14-3 Change Design Report*, Korea Rail Network Authority, Daejeon, Korea.
- Lee, C.J., Jeon, Y.J., Kim, S.H. and Park, I.J. (2016), "The influence of tunnelling on the behaviour of pre-existing piled foundations in weathered soil", *Geomech. Eng.*, **11**(4), 553-570.
- Masaki, M., Masahiro, N., Kenji, S., Motoyoshi, O. and Masashi, K. (2007), "Large double adjoined binocular tunnels at densely residential area", *Jap. Civ. Eng. Soc. Tunn. Eng. Committee*, **17**, 187-194.
- Matsuda, T. (1997), "A study on design methods for twin tunnels constructed by the single drift and central pier method", *Proc. Studies Tunn. Eng.*, 7.
- Myoung, J.W. (2008), "Stability comparison of 2-arch tunnels on excavates method", Ph.D. Dissertation, Chonnam National University, Gwangju, Korea.
- Oh, G.C. (2007), "A study on the evaluation of the loads acting on the pillar in two-arch tunnel", Ph.D. Dissertation, Hanyang University, Seoul, Korea.
- Queiroz, P.I.B., Roure, R.N. and Negro, A. (2006), "Bayesian updating of tunnel performance for Koestimate of Santiago gravel", *Proceedings of the International Symposium on Geotechnical Aspects of Underground Construction in Soft Ground*, London, U.K., June.
- Yoo, C. (2009), "Performance of multi-faced tunnelling-A 3D numerical investigation", *Tunn. Undergr. Sp. Technol.*, **24**(5), 562-573.
- Yoo, C., Kim, J.M., and Kim, H.C. (2009), "Numerical investigation on 3D behavior of 2-Arch tunnel", *J. Kor. Tunn. Undergr. Sp. Assoc.*, **11**(3), 255-264.
- Yoo, C. (2016), "Effect of spatial characteristics of a weak zone on tunnel deformation behavior", *Geomech. Eng.*, **11**(1), 41-58.
- Zidan, F.F. and Ramadan, O.M. (2018), "A hybrid MC-HS model for 3D analysis of tunnelling under piled structures", *Geomech. Eng.*, **14**(5), 479-489.